Antiferromagnetic Artificial Neuron Modeling of Biological Neural Networks

Hannah Bradley (hbradley@oakland.edu)
Oakland University
Lily Quach
Oakland University
Steven Louis
Oakland University
Vasyl Tyberkevych
Oakland University

Research Article

Keywords: Antiferromagnets, Artificial Neuron, Artificial Neural Networks, Biological System Modeling, Neuroanatomy

Posted Date: November 22nd, 2023

DOI: https://doi.org/10.21203/rs.3.rs-3616808/v1

Additional Declarations: No competing interests reported.

Antiferromagnetic Artificial Neuron Modeling of Biological Neural Networks

Hannah Bradley[1*], Lily Quach[2], Steven Louis[3], Vasyl Tyberkevych[1]

[1*]Department of Physics, Oakland University, Rochester, 48309, Michigan, USA.
[2]Oakland University William Beaumont School of Medicine, Rochester, 48309, Michigan, USA.
[3]Department of Electrical and Computer Engineering, Oakland University, Rochester, 48309, Michigan, USA.

*Corresponding author(s). E-mail(s): hbradley@oakland.edu;
Contributing authors: lilyquach@oakland.edu; slouis@oakland.edu; tyberkev@oakland.edu;

Abstract

Replicating neural responses observed in biological systems using artificial neural networks holds significant promise in the fields of medicine and engineering. In this study, we employ ultra-fast artificial neurons based on antiferromagnetic (AFM) spin Hall oscillators to emulate the biological withdrawal reflex responsible for self-preservation against noxious stimuli, such as pain or temperature. As a result of utilizing the dynamics of AFM neurons, we are able to construct an artificial neural network that can mimic the functionality and organization of the biological neural network responsible for this reflex. The unique features of AFM neurons, such as inhibition that stems from an effective AFM inertia, allow for the creation of biologically realistic neural network components, like the interneurons in the spinal cord and antagonist motor neurons. To showcase the effectiveness of AFM neuron modeling, we conduct simulations of various scenarios that define the withdrawal reflex, including responses to both weak and strong sensory stimuli, as well as voluntary suppression of the reflex.

Keywords: Antiferromagnets, Artificial Neuron, Artificial Neural Networks, Biological System Modeling, Neuroanatomy

1 Introduction

Human behavior, physiological function, and anatomical performance are all governed by the neurons running throughout our bodies. These neurons collectively form the central nervous system, encompassing the brain and spinal cord, as well as the peripheral nervous system, which establishes connections between the central system and the rest of the body (Thau et al., 2023). The interconnections between the peripheral and central nervous systems are highly complex, presenting significant challenges in comprehending their intricate mechanisms.

Many works have focused on modeling various biological neural networks connecting the peripheral and central nervous systems, aiming to deepen our understanding of their complex mechanisms (Dalcin et al., 2005, Stienen et al., 2007, Sun et al.,

ORCID: Hannah Bradley:0000-0001-9208-4827
Steven Louis: 0000-0002-6256-6005
Vasyl Tyberkevych: 0000-0002-8374-2565

2022). Artificial recreations of biological neural networks can, in principle, be used to restore sensations lost by individuals with sensory loss caused by neuronal damage. Artificial neural networks also offer the potential for medical prosthetics to exhibit sensations and actions, both voluntary and involuntary, that closely resemble those of biological systems.

Additionally, implementing realistic artificial neural networks in modern electronics holds the potential to further the development of bioinspired artificial intelligence and robotics (Bao et al., 2022, Folgheraiter and Gini, 2004, He et al., 2020, Payra et al., 2020, Wang et al., 2022). By studying neuroscience, it is possible that the next generation of behavior-based robotics could interact with their environment and demonstrate self-preservation capabilities similar to that of humans. Furthermore, bio-inspired artificial neural networks offer advantages such as reduced power consumption and high-speed training, which could revolutionize the future of robotics.

In order to replicate the connections found in human bodies, these models use artificial neurons designed to function similarly to their biological counterparts. For example, biological neurons generate voltage spikes known as action potentials in response to external stimuli that surpass an intensity threshold. Artificial neurons strive to replicate these action potentials through similar voltage spikes that are generated only after a threshold is surpassed. Current neuromorphic chips use silicon-based transistors as spiking artificial neurons (Davies et al., 2018). However, these neurons lack features that make biological neurons unique, such as spike profile, response latency, inhibition, and refractory periods.

Recent years have seen a growing interest in the use of spintronic devices as artificial neurons (Grollier et al., 2020, Ismael Salinas et al., 2023). Compared to conventional transistor-based neurons, spintronic-based neurons present many advantages. Most notably, their main advantage is that they can be made on a nanometer scale, and each device may serve as a single neuron. As a result, spintronic neuromorphic hardware has the potential to be significantly more efficient by reducing area and power consumption. The creation of artificial neurons has been shown to be possible with domain wall motion (Brigner et al., 2019, Hassan et al., 2018, Wang et al., 2023), skyrmions (Chen et al., 2018, Li et al., 2017) , spin-torque nano oscillators (Sengupta et al., 2016, Torrejon et al., 2017, Zahedinejad et al., 2020), and magnetic tunnel junctions (Cai et al., 2019, Rodrigues et al., 2023, Ross et al., 2023).

A recently proposed design for artificial neurons utilizing antiferromagnetic (AFM) spin Hall oscillators shows promise in replicating crucial characteristics of biological neurons (Bradley et al., 2023a, Khymyn et al., 2018). The unique features of AFM artificial neurons make them an excellent candidate for modeling biological neural networks. In addition to AFM neurons, it has been shown that synthetic AFM structures (Liu et al., 2020) and spin torque nano-oscillators (Louis et al., 2022) can also exhibit characteristics that closely resemble those of biological neurons.

In this work, we used the theoretical model of AFM neurons to simulate the biological neural networks responsible for the withdrawal reflex. The withdrawal reflex is a polysynaptic spinal reflex that protects the body from noxious, or harmful, stimuli (Derderian et al., 2023). Simulating withdrawal reflex mechanisms consists of five distinct scenarios: muscle tone, voluntary movement, responses to both weak and strong sensory stimuli, and the inhibition of reflexes. Our simulations demonstrate the high effectiveness of AFM neurons in reproducing responses of biological neural networks to various stimuli. To a large extent, this stems from the inertial properties of AFM neurons and is related to the possibility of a simple implementation of inhibitory neural connections (Khymyn et al., 2017), which are vital for many biological functions. As a result, the five distinct scenarios of the withdrawal reflex can be simulated with the AFM neural circuit containing less than 50 neurons.

2 Methods

2.1 The withdrawal reflex

The withdrawal reflex is a polysynaptic spinal reflex that responds to noxious or painful stimuli by stimulating the flexion of agonist muscles and inhibiting the extension of antagonist muscles of the same limb (Derderian et al., 2023). By contracting one muscle and relaxing the opposing

one, the withdrawal reflex removes a limb from the harmful stimulus.

The withdrawal reflex neural network, known as the reflex arc, involves neural pathways through the spinal cord. The reflex arc consists of sensory neurons, interneurons, and motor neurons. Sensory neurons respond to the environment by outputting spike trains with different frequencies. Interneurons in the spinal cord are able to stimulate muscles without the need for signals to travel to the brain, thereby enabling a more rapid response. Motor neurons control the muscles causing either contraction or relaxation.

Sensory neurons are part of the peripheral nervous system and are known as nociceptors, which alert the body to painful stimuli from the environment (Dubin and Patapoutian, 2010). The neurons react to a noxious stimulus by creating a train of action potentials, where the frequency of the spike train is used to encode the strength of the stimulus. Through this frequency encoding, a high-frequency spike train means a more painful and damaging stimulus (Institute of Medicine , US).

The critical components of the withdrawal reflex neural network are the excitatory and inhibitory interneurons located within the spinal cord (Purves et al., 2001). These interneurons play a pivotal role by either stimulating or inhibiting the motor neurons, thereby triggering muscle contraction or relaxation.

Finally, motor neurons are categorized into two types: agonist neurons, responsible for muscle contraction, and antagonist neurons, which induce inhibitory signals, leading to muscle relaxation (Latash, 2018). The simultaneous contraction and relaxation of the muscles cause the limb to move in one direction. The collective operation of several neurons and the existence of different response regimes make the withdrawal reflex very interesting for simulations.

In the absence of external sensory stimulus, the muscle must still remain engaged. To keep the muscles engaged and ready for movement, the brain constantly sends signals to the motor neurons; this is called the tone (Carpenter and Reddi, 2012, Ganguly et al., 2021). Muscle tone is a constant muscular activity that is a necessary background for actual movement. The tone stems from the autonomic nervous system, which is a collection of nerves alongside the brain that will fire signals to maintain muscle functionality.

In order to gain a comprehensive understanding of the withdrawal reflex, it is essential to compare it with a control scenario. This control scenario corresponds to uninterrupted voluntary limb movement. In the absence of sensory input, the brain emits signals to the motor neurons, eliciting coordinated muscle contractions and relaxations, consequently resulting in limb movement.

Similar to many neuronal pathways, the initiation of the withdrawal reflex relies on sensory neurons responding to environmental stimuli. Sensory neurons transmit signals to the brain and spinal cord after receiving stimulation from the environment. Weak sensory input, corresponding to a nonharmful stimulus, will be sent to the brain, which, in turn, will stimulate the motor neurons to move the limb. In contrast, if the sensory input is strong, as in the case of a very painful stimulus, the information will bypass the brain and travel through a shorter, faster path via the spinal interneurons. The interneurons will then directly stimulate the motor neurons, causing limb movement and triggering a much faster involuntary withdrawal response (Derderian et al., 2023).

The inhibition of a reflex is the last scenario that makes the withdrawal reflex unique and interesting to study. Biological neurons can be suppressed by a second input through inhibitory synapses, which reduces the likelihood of a neuron firing by reducing the membrane voltage further away from the threshold (Baars and Gage, 2010, Markram et al., 2004). As a result, even if the sensory signal is strong enough to trigger the withdrawal reflex through the interneurons, the cortical neurons of the brain possess the capability to inhibit these interneurons, resulting in the voluntary suppression of the reflex. To fully counteract the reflex, the brain must send voluntary signals to the motor neurons, causing the opposite reaction in the muscles; the agonist muscles relax while the antagonist muscles contract. Now, rather than being pulled away from the harmful stimulus, the limb remains in contact with it. An example of voluntary suppression of the withdrawal reflex is purposely placing one's hand on a hot stove, despite the pain and heat sensory information transmitted from sensory neurons to the brain. While difficult, higher-level impulses

from the brain have the capacity to alter reflex responsiveness.

The collective operation of multiple neurons, and the existence of five different response regimes, make the dynamic modeling of the withdrawal reflex neural network interesting but challenging to study. In this paper, we will show, via numerical simulations, that AFM neurons are capable of fully modeling all aspects of the withdrawal neural network.

2.2 AFM neurons

The artificial neurons used in this work are based on antiferromagnetic (AFM) spin Hall oscillators operating in a sub-critical regime. A detailed study of AFM oscillators, neurons, and simple AFM neural networks was presented in Refs. (Bradley et al., 2023a,b, Consolo et al., 2021, Khymyn et al., 2017, 2018). Below, we present a brief overview of AFM neurons necessary for understanding our simulation results.

Antiferromagnets are magnetically ordered materials having two magnetic sublattices oriented in opposing directions. AFM neurons employ antiferromagnets with dominant easy-plane anisotropy, for which the magnetic sublattices can relatively freely rotate in one "easy" plane, and their orientation can be described by one angle, $\phi(t)$, in this plane. If an AFM material is in contact with a layer of heavy metal (Pt in our simulations) carrying electrical current I, the spin Hall effect (Daniels et al., 2015, Khymyn et al., 2017, Sulymenko et al., 2017) creates a torque that rotates the AFM sublattices in one direction. Taking into account magnetic damping and anisotropy in the easy plane of the AFM, the dynamics of the magnetization angle $\phi(t)$ can be described by the equation,

$$\frac{1}{\omega_{ex}}\ddot{\phi} + \alpha\dot{\phi} + \frac{\omega_e}{2}\sin(2\phi) = \sigma I. \qquad (1)$$

In this equation, ω_{ex} is the exchange frequency, α is the dimensionless Gilbert damping parameter, ω_e is the characteristic anisotropy frequency, I is the bias electric current in the heavy metal layer, and σ is the proportionality coefficient determined by the geometry and material properties of the AFM neuron (Bradley et al., 2023a, Khymyn et al., 2018). In our simulations presented in this work, we used parameters typical for an AFM neuron made of NiO antiferromagnet: $\omega_{ex} = 2\pi \times 2.75$ THz and $\omega_e = 2\pi \times 1.75$ GHz (Bradley et al., 2023a).

Equation (1) closely resembles the equation of a mechanical pendulum under a driving force (Khymyn et al., 2017). Thus, the first term of the left-hand side of Eq. (1), $(1/\omega_{ex})\,\ddot{\phi}$, is equivalent to the inertial term $m\ddot{x}$ in the mechanical pendulum equation. The effective mass of the AFM, $m \propto 1/\omega_{ex}$ arises due to the exchange interaction between the AFM magnetic sublattices. It should be noted that AFM inertia is extremely important for the operation of AFM neurons. It leads to a delay between a neuron receiving input and the resulting output, an effect not found in conventional artificial neurons. The effective inertia leads to features of AFM neurons that resemble the characteristics of biological neurons, such as response latency, refraction, inhibition, and bursting (Bradley et al., 2023a). Mechanical analogs to the second term, damping, and third term, anisotropy, are, respectively, viscous friction and gravity force. These terms create a preferred orientation (anisotropy) for a mechanical pendulum. Finally, the σI term in the right-hand side of Eq. (1) describes constant torque created by the spin Hall effect.

The mechanical analogy allows one to intuitively understand AFM dynamics described by Eq. (1) on a qualitative level. Thus, when the bias current I exceeds the threshold value, $I_{th} = \omega_e/2\sigma$, needed to overcome the anisotropy ω_e, the AFM sublattices will continuously rotate in the easy plane. This supercritical regime corresponds to the oscillator regime of the AFM dynamics (Khymyn et al., 2017) and it will be used in our simulations of biological networks to generate spike trains emitted by sensory neurons and the brain.

In contrast, AFM neurons can also operate in the subcritical regime $\zeta = I/I_{th} < 1$, when the bias current alone is insufficient to overcome the AFM anisotropy. However, if an additional current pulse is applied to the neuron, the AFM magnetizations can overcome the anisotropy energy barrier and perform one rotation, during which the neuron generates a spin-pumping voltage spike proportional to the rotation speed,

$$V = \beta\dot{\phi}, \qquad (2)$$

where the efficiency $\beta = 0.11\times10^{-15}\ V\cdot s$ is defined by Eq. (2) in Bradley et al. (2023a). This response

of the AFM neuron closely resembles those of biological neurons. However, due to fast AFM dynamics, the typical duration of a spike produced by AFM neurons is a few picoseconds (see Figs. 2-4 below), which favors the use of this type of artificial neurons for ultra-fast neuromorphic applications.

The output spike generated by one AFM neuron can serve as input for other neurons if they are connected by artificial "synapses." The dynamics of such an AFM neural network is governed by the system of equations similar to Eq. (1) with additional terms describing neural connections:

$$\frac{1}{\omega_{ex}}\ddot{\phi}_i + \alpha\dot{\phi} + \frac{\omega_e}{2}\sin(2\phi) = \sigma I + \sum_{k\neq i}\kappa_{ik}\dot{\phi}_k. \quad (3)$$

Here, $\phi_i(t)$ is the phase of the i-th neuron, and κ_{ik} represents a matrix of synaptic coupling coefficients.

2.3 The Hodgkin-Huxley comparison

Unlike many conventional artificial neurons, AFM neurons have a number of features that closely resemble biological neurons, such as spike profile, response latency, and refraction time (Bradley et al., 2023a, Khymyn et al., 2018). Therefore, it is interesting to compare the AFM neuron model to a model describing a biological neuron. The Hodgkin-Huxley model is a mathematical model that describes how action potentials in biological neurons propagate (Hodgkin and Huxley, 1952). This model treats each component of biological neurons as an electrical element and has the form,

$$C_m\frac{dV_m}{dt} + g_l(V_m - V_l) + g_K(V_m - V_K) + g_{Na}(V_m - V_{Na}) = I, \quad (4)$$

where I is the total membrane current, C_m is the membrane capacitance, g_{Na} and g_k are the potassium and sodium conductance, V_K and V_{Na} are the potassium and sodium reversal potentials, respectively, g_l and V_l are the leak conductance and leak reversal potential, respectively, V_m is membrane voltage, and t is time.

A relation between the terms in Eq. (1), which describe the dynamics of the AFM neurons, and the terms in the Hodgkin-Huxley model, Eq. (4), can be made.

The membrane voltage in the Hodgkin-Huxley equation, V_m, is equivalent to the angular velocity, $\dot{\phi}$, in the AFM neuron equation because the velocity of the sublattices is used to calculate the output voltage of a neuron through Eq. (2). This implies that the first term of Eq. (4), where the derivative of V_m is taken, is analogous to the first term of Eq. (1), which has a second derivative of ϕ. Thus, the membrane capacitance, C_m, is the inertial term in the Hodgkin-Huxley equation and is equivalent to the exchange energy term, $1/\omega_{ex}$, in the AFM neuron equation.

The second term in Eq. (4), g_l, describes the leakage of ions away from the neuron. This leaky current represents the resistance in the membrane voltage as it builds to the threshold resulting in a delay of the action potential spike. This serves the same purpose as the Gilbert damping term in Eq. (1), α. Both terms include the voltage of the neuron and serve to slow the progress of a spike.

The total membrane current, I, on the right-hand side of Eq. (4), is equivalent to the coupling term on the right-hand side of Eq. (3), κ_{ik}. The membrane current in the Hodgkin-Huxley equation is the impulse into the neuron that starts the flow of ions and the build to an action potential. This corresponds to the coupling between AFM neurons, where the output of one neuron serves as the above threshold pulse to elicit another action potential in the next neuron.

The critical components of the Hodgkin-Huxley equation are the ionic conductance, g_k and g_{Na}. The opening of the ionic channels starts the production of an action potential, and when the threshold voltage is reached, the channels close, and the action potential is fired. The conductances react to the membrane voltage, V_m, with a delay, and therefore we can think of them as reacting to the integral of the membrane voltage. The flow of ions in these two channels is what prompts the start of an action potential and what causes the spike profile. This relates to the anisotropy term next to ϕ in the AFM neuron equation in Eq. (1), $\frac{\omega_e}{2}\sin(2\phi)$. The anisotropy is responsible for accelerating the AFM sublattices through the easy axis and decelerating them through the hard axis.

This acceleration and deceleration are what produce the profile of the spin-pumping voltage spike. Therefore, it is clear that the ionic conduction in the Hodgkin-Huxley equation, Eq. (4), is equivalent to the anisotropy term in the AFM neuron equation, Eq. (1).

2.4 The withdrawal reflex neural network

The architecture of the AFM neural network realizing the withdrawal reflex is shown in Fig. 1(a). It consists of the sensory neuron, the interneurons in the spinal cord, the motor neurons, and an AFM network simulating brain function. In Fig. 1, circles represent neurons and arrows represent synaptic connections determined by κ in Eq. (3).

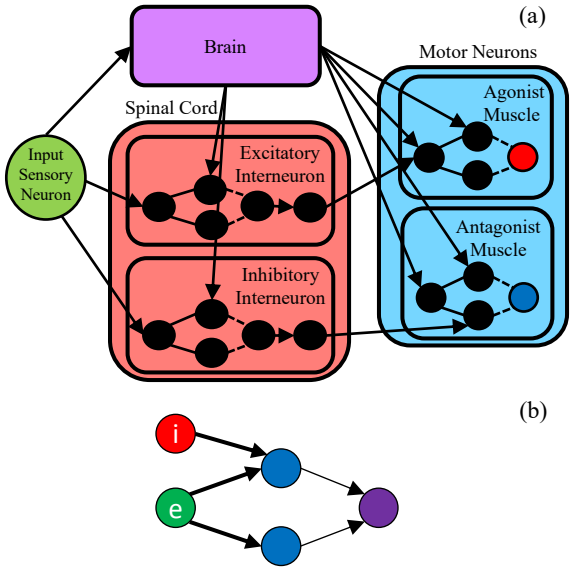

Fig. 1 (a) Architecture of the AFM withdrawal reflex artificial neural network. The network comprises two interneurons and two motor neurons constructed using inhibitor circuits. The sensory neuron is a single AFM neuron operating in a supercritical regime with variable bias current controlling the frequency of generated spike train. The architecture of the AFM neural network that simulated brain functions was different in different scenarios described in the text. (b) Inhibitor circuit.

A single AFM neuron can be excited similarly to biological neurons through a positive stimulus and results in an output of a similar voltage spike. However, a single AFM neuron lacks the ability to be suppressed in the same way biological neurons are able to. In order to act as a single biological neuron, multiple AFM neurons are connected in a so-called inhibitor circuit (Bradley et al., 2023a), shown in Fig 1(b). Here, the green excitatory neuron, labeled with an 'e', is able to send a single signal through two channels to excite the purple output neuron resulting in a spike train. However, if the inhibitory red neuron, labeled with an 'i', fires at the same time as the green excitatory neuron, the output would be suppressed, and the purple output neuron would not fire. This is due to the weakened coupling between the blue intermediate neurons and the purple output neuron. This circuit can now act as a biological neuron model with the ability to both be excited and inhibited.

The AFM input sensory neuron, the green circle in Fig. 1(a), simulates a nociceptor where the frequency of the spike train encodes the severity of sensory signal, with a higher frequency being a more painful stimulus. In our simulations, the sensory neuron was realized as a single AFM neuron operating in a supercritical regime, i.e., it had the driving current I above the threshold of self-generation I_{th} and continuously produces a spike train at a frequency that is proportional to the current (Khymyn et al., 2017, 2018). As the driving current increases, the frequency of spikes also increases, enabling the sensory neuron to simulate high-frequency sensory signals for a strong and painful stimulus and low-frequency sensory signals for a weak stimulus. For simulations without sensory inputs (tone and voluntary motion), the sensory neuron is in the subcritical regime where the bias current is reduced below the generation threshold and no spike train is produced.

Similar to the biological neural network, the AFM neural network also contains excitatory and inhibitory interneurons, lying in the pink box representing the spinal cord in Fig. 1(a) (Purves et al., 2001). The interneurons receive exciatory input from the sensory neuron. It should be noted that the interneurons are constructed from the inhibitor circuit where the inhibitory signal originates from the "brain" network, which allows for the suppression of the withdrawal reflex. The weakened coupling of the inhibitor circuits prevents low-frequency signals, stemming from the sensory neuron, from propagating through the interneurons, ensuring that the withdrawal reflex

is triggered exclusively by high-frequency, painful sensory signals. This is highly representative of the withdrawal reflex from a physiological standpoint because only noxious stimuli will elicit neuronal action potentials at a frequency and severity that will initiate the biological withdrawal reflex. A strong sensory stimulus causes the excitatory interneuron to send exciting signals to the agonist motor neurons, stimulating muscle contractions. At the same time, the inhibitory interneurons send inhibition signals to antagonist motor neurons, leading to muscle relaxation. As a result, the involuntary withdrawal reflex is triggered by a strong sensory stimulus traveling through the interneurons, causing simultaneous contraction and relaxation of the muscles, moving the limb away from the harmful stimulus.

Inhibitor circuits are also found in the construction of the antagonist and agonist motor neurons, located in the blue box in Fig. 1(a). In this way, both the brain and interneurons can send exciting signals for muscle contractions and inhibition signals for muscle relaxations. The red neurons output will determine if the agonist muscles were excited or inhibited and the blue neurons output will determine the antagonist muscles reaction.

At present, it is impossible to dynamically simulate a human brains operation. Therefore, the AFM neural network modeled brain, the purple box in Fig. 1(a), functions differently in different simulated scenarios. Actions independent of the sensory input (e.g., voluntary limb motion) were modeled using supercritical neurons generating continuous spike trains, similar to the sensory neuron. To simulate the brain reaction to a weak stimulus, we used a long chain of neurons that acted as a delay line from the sensory neuron to the motor neurons. Consequently, there is an increase in the time delay between the neural network receiving the stimulus and the brain's signal to the muscles.

3 Results and Discussion

Using the AFM neural network shown in Fig. 1(a), five different scenarios that define the withdrawal reflex were simulated. These five scenarios included tone, voluntary motion, response to a weak stimulus, response to a strong stimulus, and reflex inhibition.

3.1 Tone

Muscle tone is an essential part of any muscle motion, voluntary or involuntary. To enhance the realism of the withdrawal reflex simulation, the AFM neural networks brain component will consistently transmit a low-frequency signal to the motor neurons, replicating the effect of muscle tone.

The results of simulations of this regime are shown in Fig. 2(a) and (b). The top panel, Fig. 2(a), shows an example of the purple spike train continuously generated by the brain network and transmitted to the motor neurons in this scenario. The bottom panel, Fig. 2 (b), shows the reaction of the red agonist motor neuron (red curve) and blue antagonist motor neuron (blue curve) to the tone signal; as one can see, both motor neurons are weakly and equally excited in this case. These excitations lead to both agonist and antagonist muscles being slightly contracted, resulting in no movement yet maintaining muscle tone.

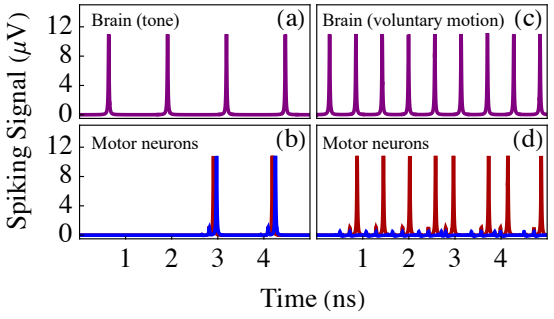

Fig. 2 Withdrawal reflex simulations in the absence of the sensory stimulus: (a-b) tone and (c-d) voluntary motion. The top row shows the neural signals generated by the brain, purple spike trains, and the bottom row shows the response of motor agonist (red line) and antagonist (blue) neurons.

3.2 Voluntary motion

The second simulated scenario is the voluntary limb motion (see Fig. 2(c-d)). Similar to the tone simulations, the voluntary motion regimen has no sensory input (the AFM sensory neurons driving current is set to 0). To simulate the conscious decision to move the limb, the motor neurons receive a purple spike train from the brain via an AFM neuron with a driving current that exceeds the

threshold (Fig. 2(c)). The signal sent by the brain causes the red agonist motor neurons to spike and the blue antagonist motor neurons to not spike, as illustrated by Fig. 2(d). The behavior of the motor neurons leads to muscle motion. A spike sequence indicates an excited motor neuron and, therefore, a simulated muscle contraction, whereas the absence of spikes indicates the suppression of a motor neuron and simulated muscle relaxation. From Fig. 2(d), it is clear that the agonist muscles (red) contract while the antagonist muscles (blue) relax, resulting in the limb's movement.

It is important to emphasize that the presence of the additional "motion" signal from the brain not only increased the spiking frequency of the agonist motor neuron but also completely suppressed the antagonist motor neuron. Such inhibitory behavior is ubiquitous in biological neural networks and vital for their proper functioning but is rather challenging to realize in conventional neural artificial networks without employing negative coupling weights. In our case, it is achieved by using simple inhibitor circuits, which are possible due to the inertial properties of AFM (Bradley et al., 2023a). This demonstrates that artificial AFM neurons are very well suited for simulations of biological neural networks and other systems with multiple competing signals.

3.3 Reaction to weak and strong stimuli

The next considered scenarios are the motor neurons response to weak and strong sensory stimuli. The results of simulations of these two scenarios are illustrated in Fig. 3.

As a result of weak and strong stimuli, the green AFM sensory neuron enters the supercritical oscillator regime, where the driving current is above the threshold. In this regime, the frequency of the spike trains generated by the neuron is proportional to the magnitude of the driving current.

Figure 3(a) shows the green sensory neuron's output for a weak sensory stimulus, while Fig. 3(c) shows a strong sensory stimulus. The strength of the stimulus is determined by the frequency of the spike train produced by the sensory neuron, with the strong and, therefore, more painful stimulus

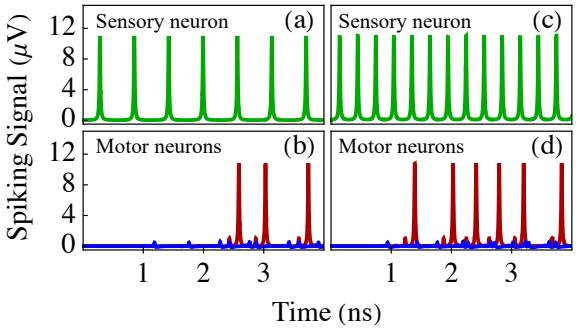

Fig. 3 Stimulated response of the withdrawal reflex arc to weak and strong sensory stimuli. (a) Spike train output of the AFM sensory neuron with a low frequency of 1.75 GHz (interspike delay 570 ps), indicating a weak stimulus. (b) Response of the motor neurons to the weak sensory stimulus. (c) Spike train output of the AFM sensory neuron with a high frequency of 3.25 GHz (delay 300 ps), indicating a strong stimulus. (d) Response of the motor neurons to the strong sensory stimulus.

having a higher frequency. Biological sensory neurons encode pain similarly through this frequency encoding (Dubin and Patapoutian, 2010).

The motor neuron's response to the sensory stimulus can be seen in Fig. 3(b) and (d). Both figures show the red agonist motor neurons being excited (red curves) and causing muscle contractions, while the blue antagonist motor neurons (blue curves) are inhibited and, therefore, causing simulated muscle relaxation. As a result, the limb is moved away from the harmful stimulus. However, the response to the strong sensory stimulus, Fig. 3(d), happens over two times faster than the response to a weak sensory stimulus, Fig. 3(b).

The faster response, shown in Fig. 3(d), is caused by the involuntary withdrawal reflex and the interneurons. A weak stimulus with low frequency cannot induce excitation in the interneurons because the inhibitor circuits are weakly coupled. Consequently, a weaker or less painful sensory signal must first travel through the brain in order to reach the motor neurons, causing a significant delay between the sensory neuron's initial stimulus and the motor neurons' reaction. As in the biological response to pain, when the sensory signal is strong, indicating a painful stimulus, interneurons are activated, creating a shorter and faster pathway for the sensory signal to travel to the motor neurons.

3.4 Inhibition of the withdrawal reflex

Due to the realistic inhibition behavior of AFM neurons, it is possible to simulate another scenario: the inhibition of the withdrawal reflex. Simulations showing the interplay between the sensory neurons, the brain, and the subsequent inhibition of the withdrawal reflex in the motor neurons are shown in Fig 4.

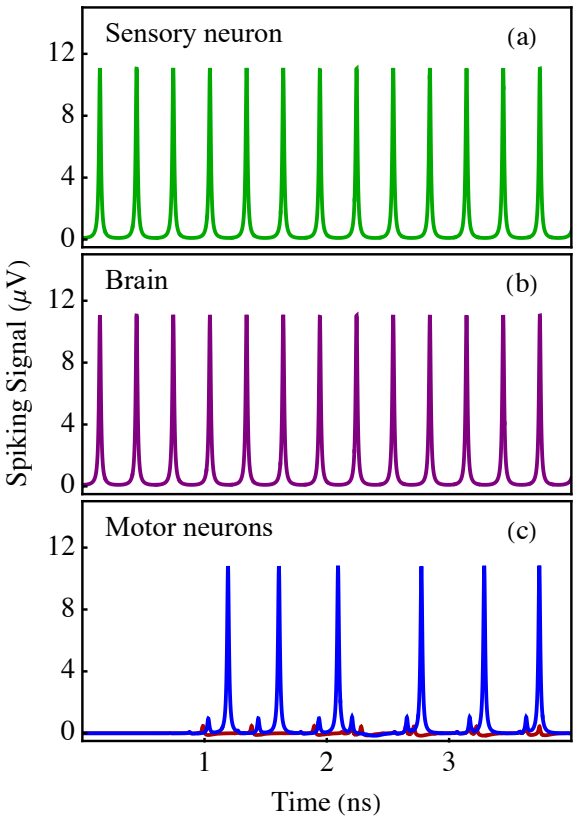

Fig. 4 Stimulated results for the inhibition of the withdrawal reflex. (a) Spike train output of the AFM sensory neuron with a high frequency of 3.25 GHz (interspike delay 300 ps), indicating a strong stimulus. (b) The signal generated by the brain to suppress the reflex. (c) Response of the motor neurons during the inhibition of the reflex regime.

In the simulations of the reflex inhibition scenario, the sensory neuron is in the strong stimulus regime, outputting a green spike train with a high frequency, as seen in Fig. 4(a), indicating a painful sensory stimulus. In normal conditions, the interneurons would be excited, and the withdrawal reflex would be triggered. In this case, however, the brain sends a voluntary purple signal to the interneurons (Fig. 4(b)), inhibiting their output and simulating a conscious decision to neutralize the reflex. It is essential that the brain triggers the opposite reaction in the motor neurons to counteract the withdrawal reflex by relaxing the agonist muscles and contracting the antagonist muscles. Figure 4(c), the response of the motor neurons, illustrates this: the blue antagonist motor neurons spike, indicating muscle contraction, and the red agonist motor neurons do not spike, indicating muscle relaxation. As a result, instead of the withdrawal reflex removing the limb away from the harmful stimulus, it stays in contact with it.

As conventional inertia-less artificial neurons cannot simulate inhibition, the ability of the AFM neuron to simulate complex inhibition adds another level of realism to the modeling of biological neural networks.

4 Conclusion

The withdrawal reflex is a complex polysynaptic spinal reflex observed in biology through its response to different strengths of sensory stimulus. By recreating the biological neural network underlying the withdrawal reflex, we enhance our understanding of its functionality and unlock potential applications in robotics. The distinct resemblance of artificial neurons derived from AFM oscillators to their biological counterparts positions them as excellent candidates for the representation of biological neural networks. Due to the realistic inhibition of AFM neurons, critical parts of the withdrawal reflex neural networks, like the inhibitory interneurons and antagonist muscles, can be accurately replicated. These features would not be possible with conventional inertia-less artificial neurons. The AFM neural network effectively simulates the withdrawal reflex through the difference in the delayed response of the muscles in scenarios involving weak and strong sensory stimuli.

Many advantages arise from using AFM neurons to simulate biological systems. The action potential spikes generated by biological neurons have a duration on the order of milliseconds. In contrast, the AFM neurons used in this study have a spike width on the order of picoseconds, due to the ultra-fast, THz dynamics of AFM materials.

This implies that any device employing AFM neurons would achieve speeds significantly surpassing those of their biological counterparts, providing a distinct advantage for the future of robotics. Due to their ultra-fast dynamics, the AFM neural network is able to simulate the withdrawal reflex on the order of nanoseconds, as opposed to the biological withdrawal reflex, which takes half a second (Derderian et al., 2023).

Energy efficiency plays a pivotal role when integrating artificial neurons into any system. The energy consumption of a biological neuron during a single action potential totals 2.5×10^{-7} J (Zhu et al., 2019). Conversely, an AFM neuron with dimensions as outlined in Bradley et al. (2023a) consumes approximately 10^{-3} pJ per spike. This energy efficiency surpasses even that of conventional artificial neurons made from transistors, which report 20 pJ of energy per synaptic operation (Davies et al., 2018).

Other biologically realistic artificial neuronal networks of spinal reflexes can use over $2,000$ artificial neurons (Bashor, 1998, Stienen et al., 2007). The AFM withdrawal reflex neural network uses a total of 45 AFM neurons, most of which are hidden and used to simulate the brain. Additionally, there is no need for simulating adjustments in the synaptic weights in the AFM reflex neural network. The network's static configuration of neurons and weights effectively reproduces the withdrawal reflex without the need for synaptic training.

The use of AFM neurons in the simulation of biological systems yields neural networks that are not only faster and more energy-efficient but also require fewer neurons. The demonstrated efficacy of the withdrawal reflex neural network model serves as a promising gateway for extending AFM neuron modeling to other biological networks, offering potential applications in both medicine and engineering.

5 Declarations

5.1 Ethical Approval

This declaration is not applicable to this study.

5.2 Funding

This work was partially supported by the Air Force Office of Scientific Research (AFOSR) Multidisciplinary Research Program of the University Research Initiative (MURI), under Grant No. FA9550-19-1-0307.

5.3 Availability of data and materials

The data presented in this text can be made available by the authors at the reader's request.

References

Bernard J. Baars and Nicole M. Gage. *Cognition, brain, and consciousness: introduction to cognitive neuroscience*. Academic Press/Elsevier, Burlington, MA, 2nd ed edition, 2010. ISBN 978-0-12-375070-9. OCLC: ocn455870625.

Chao Bao, Tae-Ho Kim, Amirhossein Hassanpoor Kalhori, and Woo Soo Kim. A 3D-printed neuromorphic humanoid hand for grasping unknown objects. *iScience*, 25(4):104119, April 2022. ISSN 2589-0042. doi: 10.1016/j.isci.2022.104119.

David P. Bashor. A large-scale model of some spinal reflex circuits. *Biological Cybernetics*, 78 (2):147–157, February 1998. ISSN 1432-0770. doi: 10.1007/s004220050421.

H. Bradley, S. Louis, C. Trevillian, L. Quach, E. Bankowski, A. Slavin, and V. Tyberkevych. Artificial neurons based on antiferromagnetic auto-oscillators as a platform for neuromorphic computing. *AIP Advances*, 13(1):015206, January 2023a. ISSN 2158-3226. doi: 10.1063/5.0128530.

Hannah Bradley, Steven Louis, Andrei Slavin, and Vasyl Tyberkevych. Pattern recognition using spiking antiferromagnetic neurons, August 2023b. arXiv:2308.09071 [physics].

Wesley H. Brigner, Joseph S. Friedman, Naimul Hassan, Lucian Jiang-Wei, Xuan Hu, Diptish Saha, Christopher H. Bennett, Matthew J. Marinella, Jean Anne C. Incorvia, and Felipe Garcia-Sanchez. Shape-Based Magnetic

Domain Wall Drift for an Artificial Spintronic Leaky Integrate-and-Fire Neuron. *IEEE Transactions on Electron Devices*, 66(11):4970–4975, November 2019. ISSN 0018-9383, 1557-9646. doi: 10.1109/TED.2019.2938952.

Jialin Cai, Bin Fang, Like Zhang, Wenxing Lv, Baoshun Zhang, Tiejun Zhou, Giovanni Finocchio, and Zhongming Zeng. Voltage-Controlled Spintronic Stochastic Neuron Based on a Magnetic Tunnel Junction. *Physical Review Applied*, 11(3):034015, March 2019. ISSN 2331-7019. doi: 10.1103/PhysRevApplied.11.034015.

Roger H. S. Carpenter and Benjamin Reddi. *Neurophysiology: a conceptual approach [free web resources, with Vitalsource ebook]*. Hodder Arnold, London, 5th ed edition, 2012. ISBN 978-1-4441-3517-6.

Xing Chen, Wang Kang, Daoqian Zhu, Xichao Zhang, Na Lei, Youguang Zhang, Yan Zhou, and Weisheng Zhao. A compact skyrmionic leaky–inotetegrate–fire spiking neuron device. *Nanoscale*, 10(13):6139–6146, March 2018. ISSN 2040-3372. doi: 10.1039/C7NR09722K. Publisher: The Royal Society of Chemistry.

G. Consolo, G. Valenti, A. R. Safin, S. A. Nikitov, V. Tyberkevich, and A. Slavin. Theory of the electric field controlled antiferromagnetic spin Hall oscillator and detector. *Physical Review B*, 103(13):134431, April 2021. doi: 10.1103/PhysRevB.103.134431. Publisher: American Physical Society.

Bruno L. Dalcin, Frederico Alan Cruz, Célia Martins Cortez, and Emmanuel P. L. Passos. Computer modeling of a spinal reflex circuit. *Brazilian Journal of Physics*, 35:987–994, December 2005. ISSN 0103-9733, 1678-4448. doi: 10.1590/S0103-97332005000600013. Publisher: Sociedade Brasileira de Física.

Matthew W Daniels, Wei Guo, G Malcolm Stocks, Di Xiao, and Jiang Xiao. Spin-transfer torque induced spin waves in antiferromagnetic insulators. *New Journal of Physics*, 17(10):103039, October 2015. ISSN 1367-2630. doi: 10.1088/1367-2630/17/10/103039.

Mike Davies, Narayan Srinivasa, Tsung-Han Lin, Gautham Chinya, Prasad Joshi, Andrew Lines, Andreas Wild, Hong Wang, and Deepak Mathaikutty. Loihi: A Neuromorphic Manycore Processor with On-Chip Learning. *IEEE Micro*, PP:1–1, January 2018. doi: 10.1109/MM.2018.112130359.

Celena Derderian, Karlie R. Shumway, and Prasanna Tadi. Physiology, Withdrawal Response. In *StatPearls*. StatPearls Publishing, Treasure Island (FL), 2023.

Adrienne E. Dubin and Ardem Patapoutian. Nociceptors: the sensors of the pain pathway. *The Journal of Clinical Investigation*, 120(11):3760–3772, November 2010. ISSN 0021-9738. doi: 10.1172/JCI42843.

Michele Folgheraiter and Giuseppina Gini. Human-like reflex control for an artificial hand. *Biosystems*, 76(1):65–74, August 2004. ISSN 0303-2647. doi: 10.1016/j.biosystems.2004.05.007.

Jacky Ganguly, Dinkar Kulshreshtha, Mohammed Almotiri, and Mandar Jog. Muscle Tone Physiology and Abnormalities. *Toxins*, 13(4):282, April 2021. ISSN 2072-6651. doi: 10.3390/toxins13040282.

J. Grollier, D. Querlioz, K. Y. Camsari, K. Everschor-Sitte, S. Fukami, and M. D. Stiles. Neuromorphic spintronics. *Nature Electronics*, 3(7):360–370, July 2020. ISSN 2520-1131. doi: 10.1038/s41928-019-0360-9. Number: 7 Publisher: Nature Publishing Group.

Naimul Hassan, Xuan Hu, Lucian Jiang-Wei, Wesley H. Brigner, Otitoaleke G. Akinola, Felipe Garcia-Sanchez, Massimo Pasquale, Christopher H. Bennett, Jean Anne C. Incorvia, and Joseph S. Friedman. Magnetic domain wall neuron with lateral inhibition. *Journal of Applied Physics*, 124(15):152127, 2018. Publisher: AIP Publishing LLC.

Ke He, Yaqing Liu, Ming Wang, Geng Chen, Ying Jiang, Jiancan Yu, Changjin Wan, Dianpeng Qi, Meng Xiao, Wan Ru Leow, Hui Yang, Markus Antonietti, and Xiaodong Chen. An Artificial Somatic Reflex Arc. *Advanced Materials*, 32(4):

1905399, 2020. ISSN 1521-4095. doi: 10.1002/adma.201905399.

A. L. Hodgkin and A. F. Huxley. A quantitative description of membrane current and its application to conduction and excitation in nerve. *The Journal of Physiology*, 117(4): 500–544, August 1952. ISSN 0022-3751.

Disability Institute of Medicine (US) Committee on Pain, Marian Osterweis, Arthur Kleinman, and David Mechanic. *The Anatomy and Physiology of Pain*. National Academies Press (US), 1987. Publication Title: Pain and Disability: Clinical, Behavioral, and Public Policy Perspectives.

Rudis Ismael Salinas, Po-Chuan Chen, Chao-Yao Yang, and Chih-Huang Lai. Spintronic materials and devices towards an artificial neural network: accomplishments and the last mile. *Materials Research Letters*, 11(5):305–326, May 2023. ISSN null. doi: 10.1080/21663831.2022.2147803. Publisher: Taylor & Francis _eprint: https://doi.org/10.1080/21663831.2022.2147803.

Roman Khymyn, Vasil Tiberkevich, and Andrei Slavin. Antiferromagnetic spin current rectifier. *AIP Advances*, 7(5):055931, March 2017. ISSN 2158-3226. doi: 10.1063/1.4977974.

Roman Khymyn, Ivan Lisenkov, James Voorheis, Olga Sulymenko, Oleksandr Prokopenko, Vasil Tiberkevich, Johan Akerman, and Andrei Slavin. Ultra-fast artificial neuron: generation of picosecond-duration spikes in a current-driven antiferromagnetic auto-oscillator. *Scientific Reports*, 8(1):15727, October 2018. ISSN 2045-2322. doi: 10.1038/s41598-018-33697-0. Number: 1 Publisher: Nature Publishing Group.

Mark L. Latash. Muscle coactivation: definitions, mechanisms, and functions. *Journal of Neurophysiology*, 120(1):88–104, July 2018. ISSN 0022-3077. doi: 10.1152/jn.00084.2018. Publisher: American Physiological Society.

Sai Li, Wang Kang, Yangqi Huang, Xichao Zhang, Yan Zhou, and Weisheng ZHAO. Magnetic skyrmion-based artificial neuron device. *Nanotechnology*, 28:31LT01, July 2017. doi: 10.1088/1361-6528/aa7af5.

Yizhou Liu, Igor Barsukov, Yafis Barlas, Ilya N. Krivorotov, and Roger K. Lake. Synthetic antiferromagnet-based spin Josephson oscillator. *Applied Physics Letters*, 116(13):132409, April 2020. ISSN 0003-6951. doi: 10.1063/5.0003477.

Steven Louis, Hannah Bradley, Andrei Slavin, and Vasyl Tyberkevych. Artificial neuron based on a spin torque nano oscillator. *Book of Abstracts for 7th International Conference on Magnonics, C4–28*, 2022.

Henry Markram, Maria Toledo-Rodriguez, Yun Wang, Anirudh Gupta, Gilad Silberberg, and Caizhi Wu. Interneurons of the neocortical inhibitory system. *Nature Reviews Neuroscience*, 5(10):793–807, October 2004. ISSN 1471-0048. doi: 10.1038/nrn1519. Number: 10 Publisher: Nature Publishing Group.

Syamantak Payra, Gabriel Loke, and Yoel Fink. Enabling Adaptive Robot-Environment Interaction and Context-Aware Artificial Somatosensory Reflexes through Sensor-Embedded Fibers. In *2020 IEEE MIT Undergraduate Research Technology Conference (URTC)*, pages 1–4, October 2020. doi: 10.1109/URTC51696.2020.9668863.

Dale Purves, George J. Augustine, David Fitzpatrick, Lawrence C. Katz, Anthony-Samuel LaMantia, James O. McNamara, and S. Mark Williams. Excitatory and Inhibitory Postsynaptic Potentials. *Neuroscience. 2nd edition*, 2001. Publisher: Sinauer Associates.

Davi R. Rodrigues, Rayan Moukhader, Yanxiang Luo, Bin Fang, Adrien Pontlevy, Abbas Hamadeh, Zhongming Zeng, Mario Carpentieri, and Giovanni Finocchio. Spintronic Hodgkin-Huxley-Analogue Neuron Implemented with a Single Magnetic Tunnel Junction. *Physical Review Applied*, 19(6):064010, June 2023. doi: 10.1103/PhysRevApplied.19.064010. Publisher: American Physical Society.

Andrew Ross, Nathan Leroux, Arnaud De Riz, Danijela Marković, Dédalo Sanz-Hernández,

Juan Trastoy, Paolo Bortolotti, Damien Querlioz, Leandro Martins, Luana Benetti, Marcel S. Claro, Pedro Anacleto, Alejandro Schulman, Thierry Taris, Jean-Baptiste Begueret, Sylvain Saïghi, Alex S. Jenkins, Ricardo Ferreira, Adrien F. Vincent, Frank Alice Mizrahi, and Julie Grollier. Multilayer spintronic neural networks with radiofrequency connections. *Nature Nanotechnology*, pages 1–8, July 2023. ISSN 1748-3395. doi: 10.1038/s41565-023-01452-w. Publisher: Nature Publishing Group.

Abhronil Sengupta, Priyadarshini Panda, Parami Wijesinghe, Yusung Kim, and Kaushik Roy. Magnetic Tunnel Junction Mimics Stochastic Cortical Spiking Neurons. *Scientific Reports*, 6 (1):30039, July 2016. ISSN 2045-2322. doi: 10.1038/srep30039. Number: 1 Publisher: Nature Publishing Group.

Arno H. A. Stienen, Alfred C. Schouten, Jasper Schuurmans, and Frans C. T. van der Helm. Analysis of reflex modulation with a biologically realistic neural network. *Journal of Computational Neuroscience*, 23(3):333–348, December 2007. ISSN 1573-6873. doi: 10.1007/s10827-007-0037-7.

O. R. Sulymenko, O. V. Prokopenko, V. S. Tiberkevich, A. N. Slavin, B. A. Ivanov, and R. S. Khymyn. THz-Frequency Spin-Hall Auto-Oscillator Based on a Canted Antiferromagnet. *Physical Review Applied*, 8(6):064007, December 2017. ISSN 2331-7019. doi: 10.1103/PhysRevApplied.8.064007. arXiv:1707.07491 [physics].

Lin Sun, Yi Du, Haiyang Yu, Huanhuan Wei, Wenlong Xu, and Wentao Xu. An Artificial Reflex Arc That Perceives Afferent Visual and Tactile Information and Controls Efferent Muscular Actions. *Research*, 2022:9851843, February 2022. ISSN 2639-5274. doi: 10.34133/2022/9851843.

Lauren Thau, Vamsi Reddy, and Paramvir Singh. Anatomy, Central Nervous System. In *StatPearls*. StatPearls Publishing, Treasure Island (FL), 2023.

Jacob Torrejon, Mathieu Riou, Flavio Abreu Araujo, Sumito Tsunegi, Guru Khalsa, Damien Querlioz, Paolo Bortolotti, Vincent Cros, Kay Yakushiji, Akio Fukushima, Hitoshi Kubota, Shinji Yuasa, Mark D. Stiles, and Julie Grollier. Neuromorphic computing with nanoscale spintronic oscillators. *Nature*, 547(7664):428–431, July 2017. ISSN 1476-4687. doi: 10.1038/nature23011. Number: 7664 Publisher: Nature Publishing Group.

Depeng Wang, Shufang Zhao, Linlin Li, Lili Wang, Shaowei Cui, Shuo Wang, Zheng Lou, and Guozhen Shen. All-Flexible Artificial Reflex Arc Based on Threshold-Switching Memristor. *Advanced Functional Materials*, 32(21):2200241, 2022. ISSN 1616-3028. doi: 10.1002/adfm.202200241.

Di Wang, Ruifeng Tang, Huai Lin, Long Liu, Nuo Xu, Yan Sun, Xuefeng Zhao, Ziwei Wang, Dandan Wang, Zhihong Mai, Yongjian Zhou, Nan Gao, Cheng Song, Lijun Zhu, Tom Wu, Ming Liu, and Guozhong Xing. Spintronic leaky-integrate-fire spiking neurons with self-reset and winner-takes-all for neuromorphic computing. *Nature Communications*, 14(1):1068, February 2023. ISSN 2041-1723. doi: 10.1038/s41467-023-36728-1. Number: 1 Publisher: Nature Publishing Group.

Mohammad Zahedinejad, Ahmad A. Awad, Shreyas Muralidhar, Roman Khymyn, Himanshu Fulara, Hamid Mazraati, Mykola Dvornik, and Johan Åkerman. Two-dimensional mutually synchronized spin Hall nano-oscillator arrays for neuromorphic computing. *Nature Nanotechnology*, 15 (1):47–52, January 2020. ISSN 1748-3395. doi: 10.1038/s41565-019-0593-9. Number: 1 Publisher: Nature Publishing Group.

Fengyun Zhu, Rubin Wang, Xiaochuan Pan, and Zhenyu Zhu. Energy expenditure computation of a single bursting neuron. *Cognitive Neurodynamics*, 13(1):75–87, February 2019. ISSN 1871-4080. doi: 10.1007/s11571-018-9503-3.